

# Characteristic Mode Analysis of Wideband Microstrip Antenna

Bhaskara Rao Perli<sup>1, \*</sup> and Avula M. Rao<sup>2</sup>

**Abstract**—In this paper, a wideband antenna is designed systematically based on characteristic mode analysis (CMA). The antenna consists of a rectangle, a semi-annular ring, and a microstrip line. The radiating behavior and resonant frequencies of the radiating element are analyzed by using first four characteristic modes. First two modes only have wideband behavior and are excited by CPW feeding<sup>3</sup> technique. The proposed antenna is printed on a low cost FR4 substrate with a size of  $35 \times 50 \times 1.6 \text{ mm}^3$  and impedance bandwidth ranging from 1.6 to 3.8 GHz for the applications of GSM, DCS, LTE, and WIMAX. To validate the proposed approach, the wideband antenna is fabricated and tested. A wide impedance bandwidth of 81% with  $|S_{11}| < -10 \text{ dB}$  is achieved for both simulation and measurement results.

## 1. INTRODUCTION

Recent days, wideband antennas attract great interest in wireless services such as WiMax, WI-Fi, 2G, 3G, Long-Term Evolution (LTE), and 4G which require large impedance bandwidth and stable radiation patterns over their operating frequency range. Different approaches are available in literature to generate wideband antennas. One approach is based on the frequency independent antenna concept [1] such as conical antennas [2], log-periodic antennas [3], and spiral antennas [4]. Unfortunately, the geometrical structure of antennas [2–4] is difficult to fabricate due to their complex and bulky nature. On the other hand, microstrip patch antennas are popular candidates for providing wideband characteristics due to the low-profile structure, low cost, easy fabrication, and light weight features [5].

However, the physical insight underlying the generation of wideband remains mostly unexplored in existing literature. In this regard, the present work employs the theory of characteristic modes (TCM) of [6] to design an efficient radiating topology that provides wideband characteristics. The TCM is based on the method of moment formulation of electric field integral equation and is found to be useful in proving various antenna parameters in the literature. In recent years, different types of antennas well designed by using characteristic mode theory (CMT) for different applications are Slot antennas [7–10], MIMO antennas [11–14], UWB antennas [15–17], Platform antennas [18–21], Metasurface antennas [22–26], and Wideband antennas [27–34].

This paper aims at the design of a wideband antenna by applying the characteristic mode analysis (CMA) to the proposed antenna. The impedance bandwidth can be broadened by combining the first two characteristic modes. These two modes are simultaneously excited with simple feeding structure and have obtained good impedance matching for the band of frequency ranging from 1.6 to 3.8 GHz. The paper is organized as follows. Section 2 provides the background theory of CMA and corresponding modal attributes. Next, modal analysis of the radiating antenna is reported. Later, the design is compared with full-wave simulations, and results are discussed in details. Lastly, the work is summarized in the conclusion section.

---

Received 14 September 2019, Accepted 19 November 2019, Scheduled 12 December 2019

\* Corresponding author: Bhaskara Rao Perli (mail2bhaskarp@gmail.com).

<sup>1</sup> JNTUA, Anathapuram, India. <sup>2</sup> Department of ECE, PBRVITS, Kavali, A.P, India.

## 2. CHARACTERISTIC MODE ANALYSIS

The TCM was initially introduced by Garbacz and Turpin in [35] and was later modified in the contexts of method of moment matrix by Harrington and Mautz in the seventies [36, 37]. For arbitrarily shaped lossless structures, the TCM provides a set of real characteristic current modes which are over the MoM impedance matrix space. Corresponding characteristic field modes are orthogonal over the infinite radiation sphere. The total current on the surface of the conducting object can be expressed as a weighted sum of the characteristic current modes [38].

The characteristic modes can be used to calculate the resonance frequency of modes and provide a physical insight into antenna radiation. Each characteristic mode consists of an eigenvalue or a characteristic angle which gives the knowledge about the mode resonance and radiating behavior. The characteristic modes only depend on the size and shape of the conducting object in order to get controlled performance of the antenna design. Moreover, optimum feeding arrangement will be obtained to excite the desired modes which give the required radiating performance [39].

CMA provides the deterministic design approach, which is more efficient than a trial-and-error practice or time-consuming optimization. The CMA can be used to optimize the antenna shape and better antenna topology [40]. CMA first starts with the distributions of surface currents on the conducting body for the design or analyze the antenna structure. Next, it allows choosing the feed point and feed configuration to simulate the required characteristic mode or combination of the first few characteristic modes, and other modes are suppressed in order to obtain the desired antenna performance [41].

For a given conducting object, any electric current ( $\vec{J}$ ) on its surface can be expressed as a sum of characteristic modes or eigencurrents ( $J_n$ ) with different product coefficients ( $\beta_n$ )

$$\vec{J} = \sum_n \beta_n J_n = \sum_n \frac{V_n^i \vec{J}_n}{1 + J\lambda_n} \quad (1)$$

From Equation (1), the wideband antenna design will be evaluated with the help of three important parameters, namely the modal excitation coefficient ( $V_n^i$ ), characteristic angle ( $\beta_n$ ), and modal significance ( $MS_n$ ) as the function of eigenvalue ( $\lambda_n$ ), which are given as:

$$V_n^i = \langle \vec{J}_n, \vec{E}^i \rangle = \iint_s \vec{J}_n \cdot \vec{E}^i ds \quad (2)$$

$$\beta_n = 180^\circ - \tan^{-1}(\lambda_n) \quad (3)$$

$$MS_n = \frac{1}{1 + J\lambda_n} \quad (4)$$

The phase difference between the current mode  $J_n$  and the modal electric field  $E_n$  is well characterized by the characteristic angle, and the physical interpretation of characteristic angle was presented briefly in [35]. When  $\beta$  is for any modes close to  $180^\circ$ , those modes radiate well at their resonant frequencies, respectively; otherwise, store energy which indicates that  $\beta$  is near  $90^\circ$  or  $270^\circ$ . The modal significance is used to quantify the part of a specific mode to the total radiation when a source is applied.

### 2.1. Characteristic Mode Analysis of Proposed Antenna-1

For CMA, the proposed antenna-1 is analyzed with zero thickness of perfect conductor and without any substrate as presented in Figure 1.

The CMA of antenna-2 will be analyzed with the first four modes. It consists of the rectangle shape added with a semi-annular ring. The geometry and characteristic current distribution for the first two modes are depicted in Figure 2. From Figure 2, the current emerging from the rectangular plate of the first mode is split into two oppositely orient current distributions in the semi-ring section. From matrix block-partition concept of [42, 43], it can be thought as an odd mode or differential mode. Alternately, the direction of the current distribution of the second mode is identical throughout the semi-ring, and it can be termed as an even mode. The generation of such odd and even modes is lying on

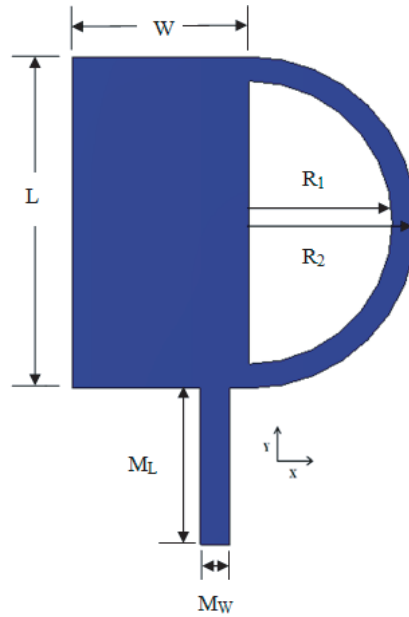


Figure 1. Geometry of proposed antenna-1.

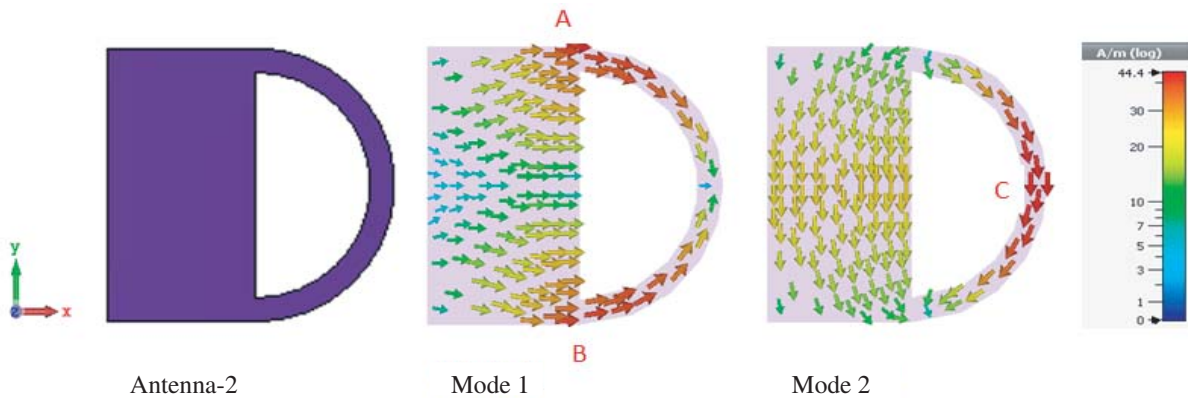


Figure 2. Geometry and surface current distribution for the modes 1–4 of the antenna-2.

the C-2v symmetry of the reference geometry. With the Galerkin’s matching, the MoM matrix becomes complex whose eigenspace is a combination of consecutive pair of odd and even modes [35, 36]. If such an adjacent pair of odd and even modes is excited simultaneously, wideband radiation characteristics can be achieved. It can be seen from Figure 2 that the first two modes have more surface current concentrated at A, B and C points.

According to Equation (1), the numerator of modal weighting coefficient is an inner product of the impressed excitation signal and modal current. So, if these two vectors are aligned parallel, corresponding mode will experience maximum strength of excitation. The optimized feed point will be at maxima of the modal current. For example, points A and B are suitable feeding locations for mode 1, while point C for mode 2 is as illustrated in Figure 2.

The characteristic angles and modal significance of the first four modes with respect to frequency are presented in Figures 3 and 4. From Figure 3, the first two modes are resonant modes which cross 180° reference axis at 3.2 GHz and 4.2 GHz. The third mode is non-resonant mode which does not cross 180° reference axis. The fourth mode resonates at some other high frequency beyond 5 GHz. From Figure 4, the first two modes occupy a large modal significance around 1, and those modes efficiently radiate around their resonant frequencies. Corresponding radiation patterns of modes 1 and 2 are reported in Figures 5(a) and 5(b).

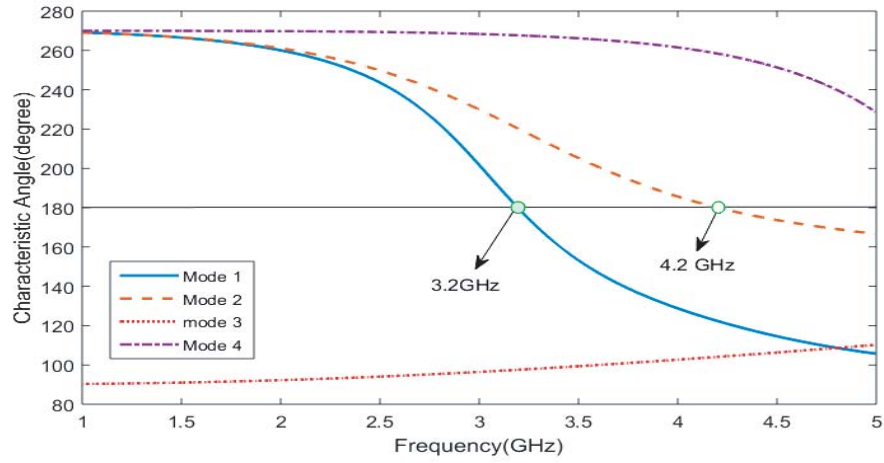


Figure 3. Characteristic angles of modes 1–4 of the antenna-2.

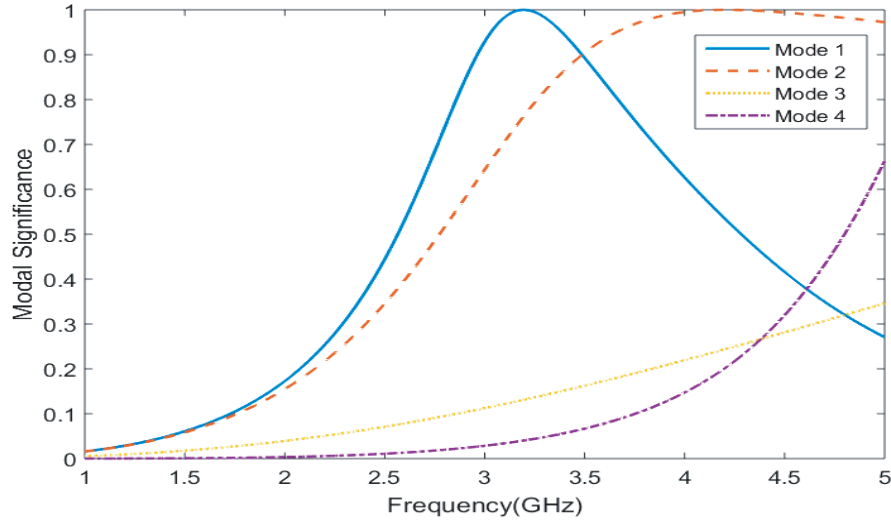


Figure 4. Modal significance of modes 1–4 of the antenna-2.

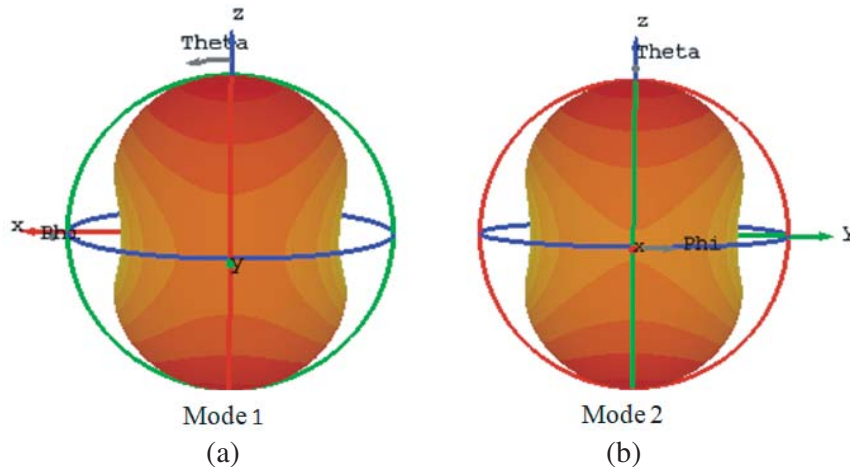
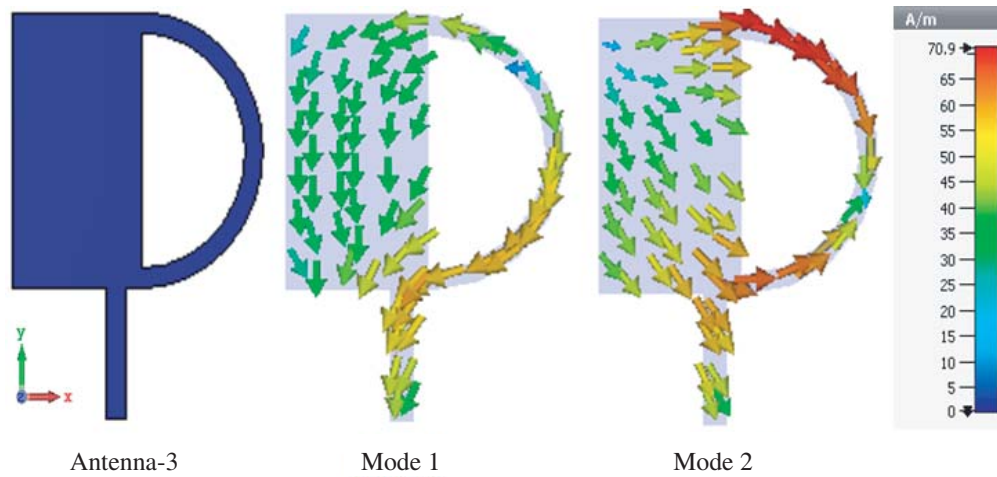


Figure 5. Radiation patterns of (a) mode 1 at 3.2 GHz, (b) mode 2 at 4.2 GHz of the antenna-2.

However, our objective is to excite both modes 1 and 2 simultaneously in order to get wideband behavior. As can be noted from Figure 2, the total current distribution is a collection of the currents from the rectangular plate and semi-ring elements. The first one produces an electric dipole type current distribution whereas the ring structure provides a magnetic dipole like current distribution. Therefore, the microstrip line is placed in the junction of these two elements such that the impressed signal can excite both the rectangular and semi-ring structures as shown in Figure 6.



**Figure 6.** Geometry and surface current distributions of mode 1 at 3.08 GHz and mode 2 at 3.3 GHz of the antenna-3.

Modes 1 and 2 are excited with suitable feeding technique through microstrip line in order to design a wideband antenna. The characteristic angles and modal significance of modes 1–4 of the radiating element with a microstrip line are illustrated in Figures 7 and 8. Now modes 1 and 2 closely resonate at 3.08 GHz and 3.3 GHz. From Figure 8, a large modal significance around 1 is occupied by the first two modes at their resonant frequencies, but modes 3 and 4 cannot be excited because their modal significance is far less than 1. These two modes will not be considered in further study. Modes 1 and 2 with their radiation patterns at 3.08 GHz and 3.3 GHz of antenna-3 are presented in Figure 9.

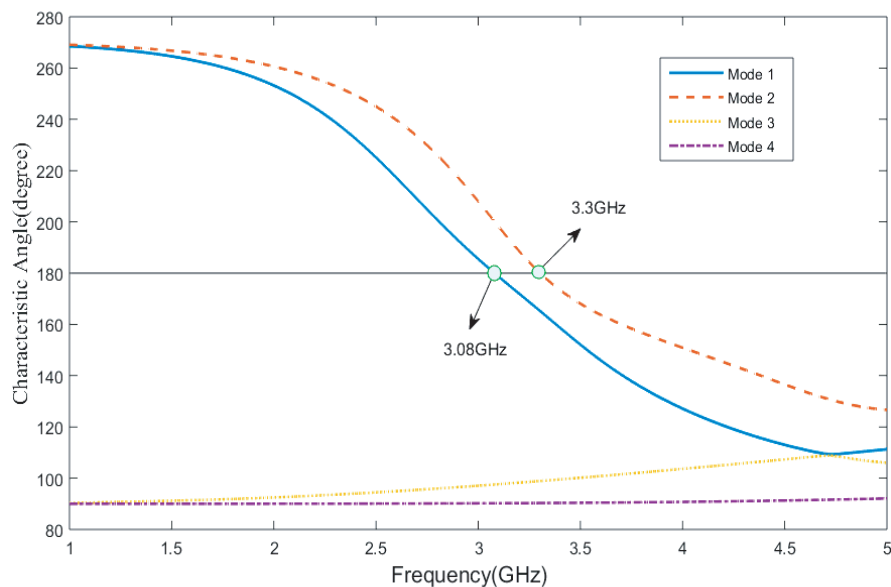


**Figure 7.** Characteristic angles of modes 1–4 of the antenna-3.

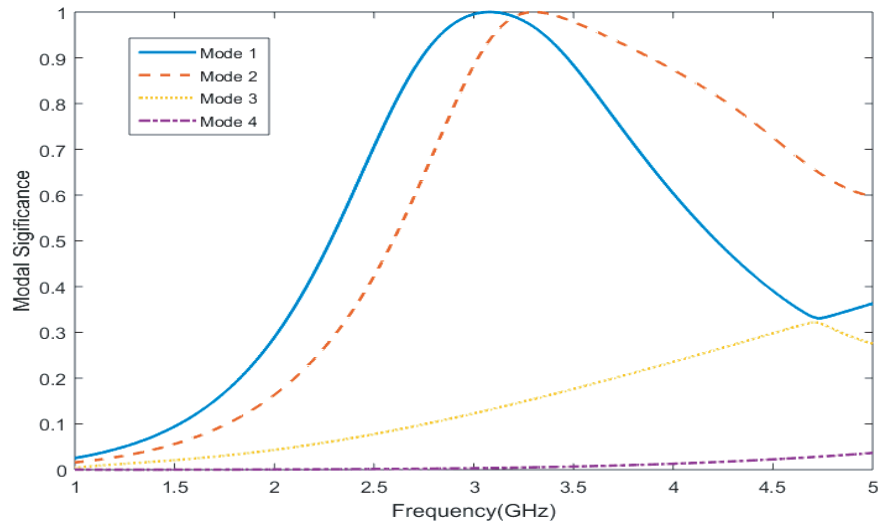


**Figure 8.** Modal significance of modes 1–4 of the antenna-3.

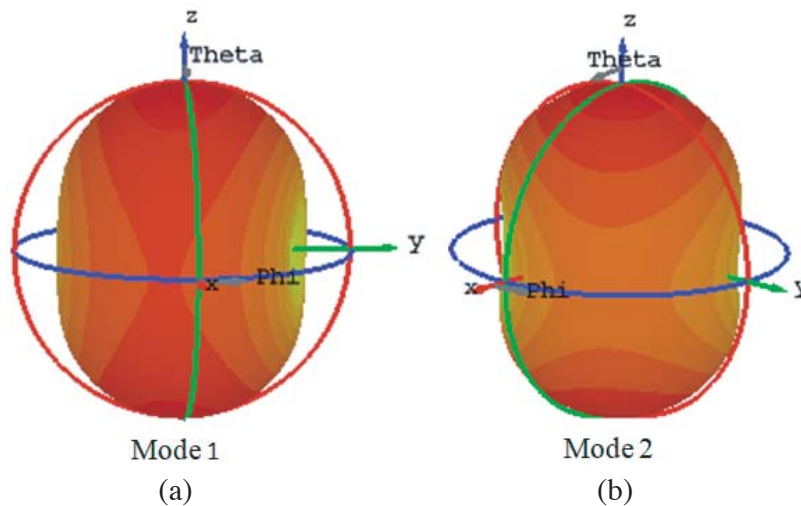


**Figure 9.** Radiation patterns of (a) mode 1 at 3.08 GHz, (b) mode 2 at 3.3 GHz of the antenna-3.

### 3. WIDEBAND ANTENNA DESIGN

Detailed dimensions of the proposed antenna are presented in Figure 10. The proposed antenna has an FR4 substrate with size of  $35 \times 50 \times 1.6 \text{ mm}^3$ ,  $\epsilon_r = 4.3$ , and  $\tan \delta = 0.02$ .

As illustrated in Figure 10, the radiating element consists of a rectangle, a semi-annular ring antenna, and a microstrip line. The rectangle, semi-annular ring antenna, and microstrip line are printed on the upper side of the substrate and defected ground also on the upper side. The optimum feeding location is selected through the microstrip line, i.e., also called the feed line. A simple CPW feeding technique is selected to excite the proposed antenna. In Coplanar Waveguide (CPW) feeding configuration, the feed width of  $M_w = 3 \text{ mm}$  and gap of  $g = 0.35 \text{ mm}$  between the coplanar ground and feed line are carefully chosen to excite the desired first two modes, i.e., modes 1 and 2 while maintaining the characteristic impedance  $50 \Omega$ . The optimized dimensions of the proposed antenna are given in Table 1.

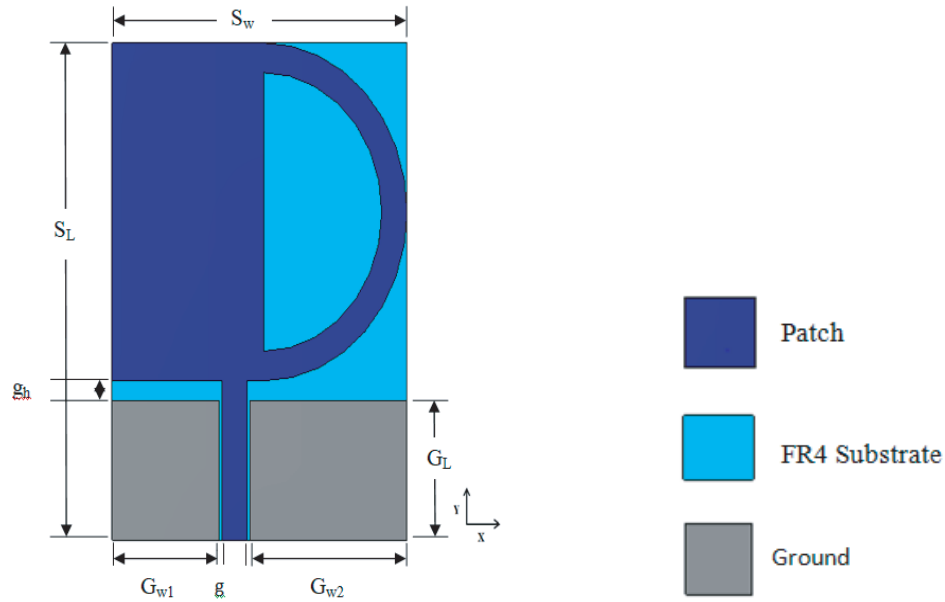


Figure 10. Proposed antenna geometry (front view).

Table 1. Proposed antenna optimized parameters.

Parameters	$S_L$	$S_w$	$L$	$W$	$G_L$	$G_{w1}$	$G_{w2}$	$g$	$g_h$	$R_1$	$R_2$	$M_L$	$M_w$
Values (mm)	50	35	34	18	14	12.65	18.65	0.35	2	17	14	16	3

### 3.1. Parametric Study

The impact of changes in the parameters, such as the length of the ground  $G_L$  and slot width of the ground  $g$  on  $S_{11}$ , is illustrated as follows.

When a single parameter is varied, remaining parameters are maintained at constant. In CPW feeding technique, the height and slot width of the ground plane play a key role to excite the first two

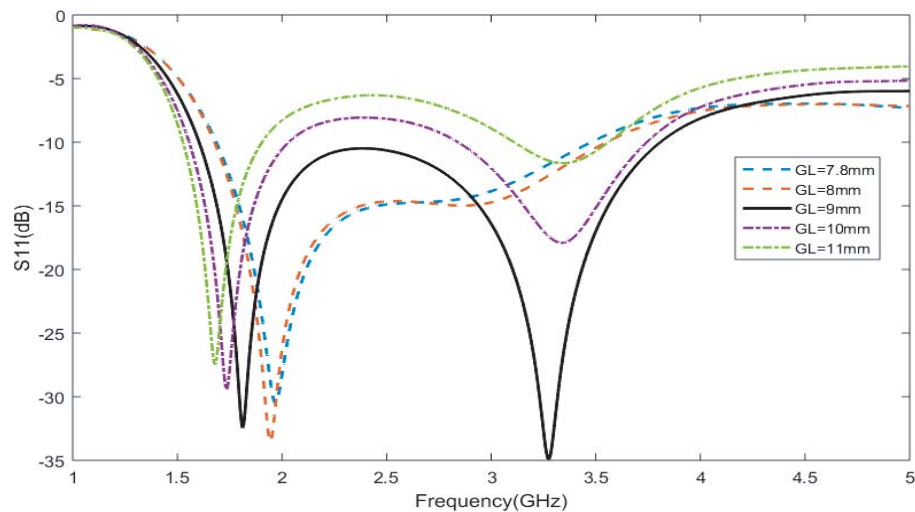
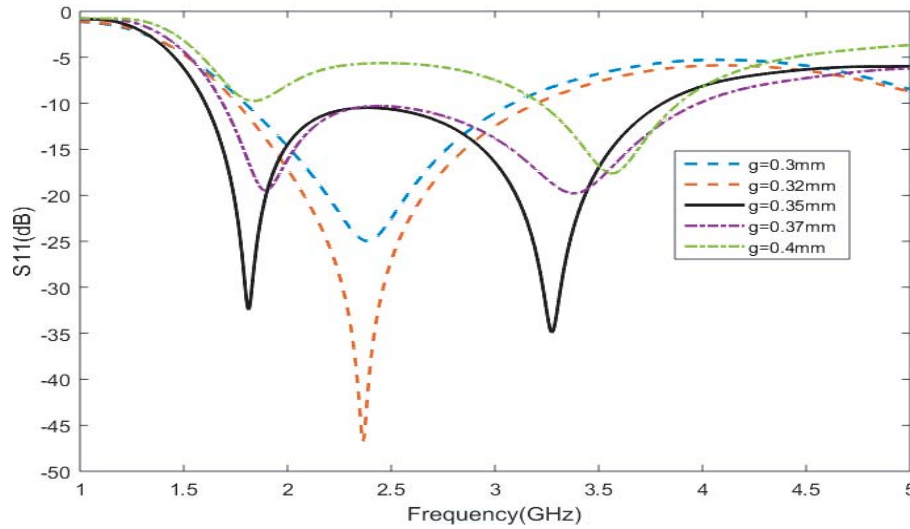


Figure 11. Effect on  $S_{11}$  with variation of  $G_L$ .



**Figure 12.** Effect on  $S_{11}$  with variation of  $g$ .

modes simultaneously. The value of  $G_L$  at 9 mm provides the two resonant frequency bands. From Figure 11, it can be observed that two resonant frequencies at 1.8 GHz and 3.3 GHz, which are related to the characteristic modes 1 and 2 as per analysis presented in Section 2. As the length of the ground plane decreases, it excites only one resonant mode while increases the length of the ground plane, two resonant modes are excited. Therefore,  $G_L = 9$  mm is the best choice for better resonance of two modes and increasing impedance bandwidth.

From Figure 12, the slot width of the ground  $g = 0.35$  mm is the best choice for better resonance of two modes and increasing impedance bandwidth. The increasing value of  $g$  has resonance of two modes while decreasing the value has resonance of only one mode.

From Figure 13, the feed width  $M_w$  is varied from 2 mm to 4 mm while maintaining the value of ground slot width  $g$  as constant. The feed width  $M_w = 3$  mm is the finest way to excite the first two modes and to get larger impedance bandwidth. As the length of the feed width  $M_w$  increases, the two modes are excited with smaller bandwidth. While it decreases, resonance of the two modes is not under good impedance matching, even though exciting two modes.

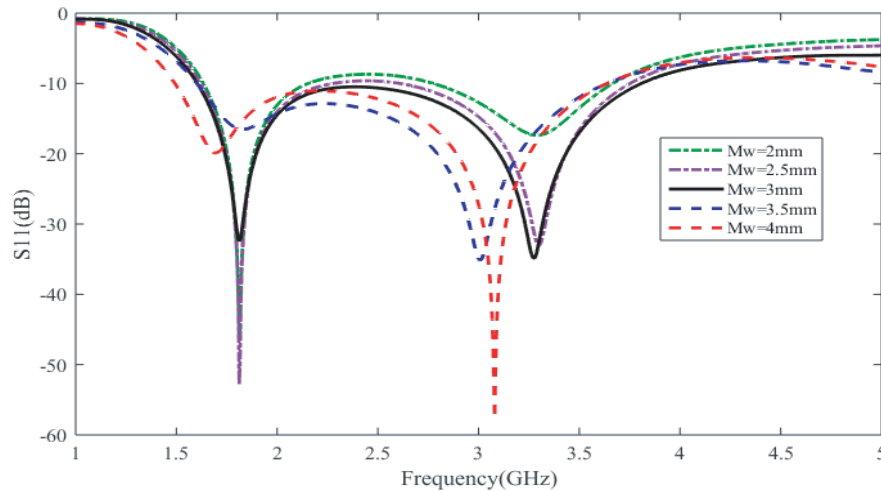


**Figure 13.** Effect on  $S_{11}$  with variation of  $M_w$ .

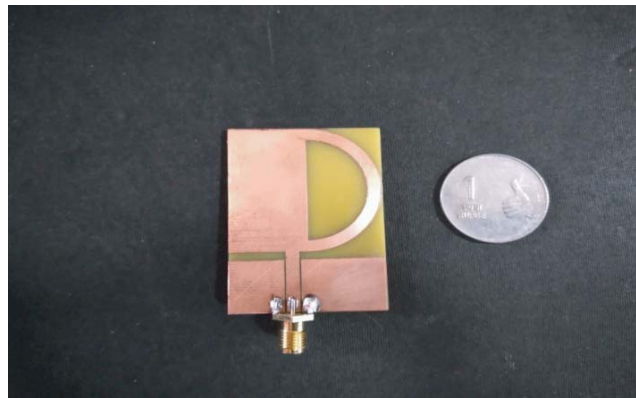


Figure 14. Fabricated antenna (top view).

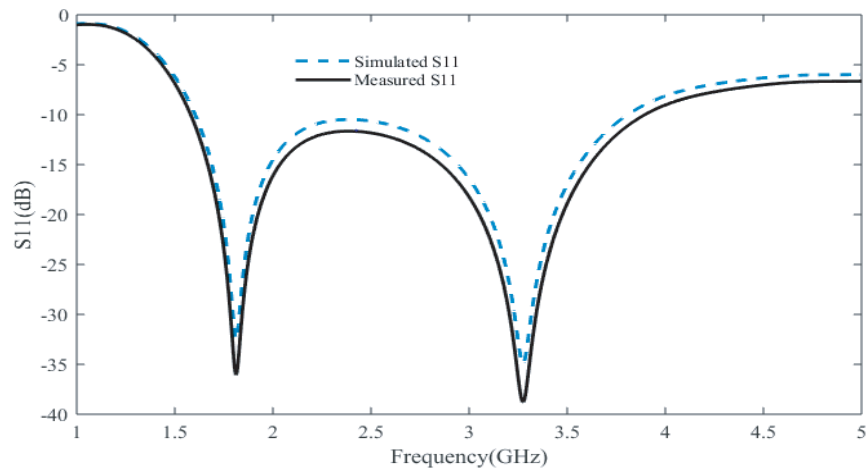


Figure 15. Simulated and measured reflection coefficient of the proposed antenna.

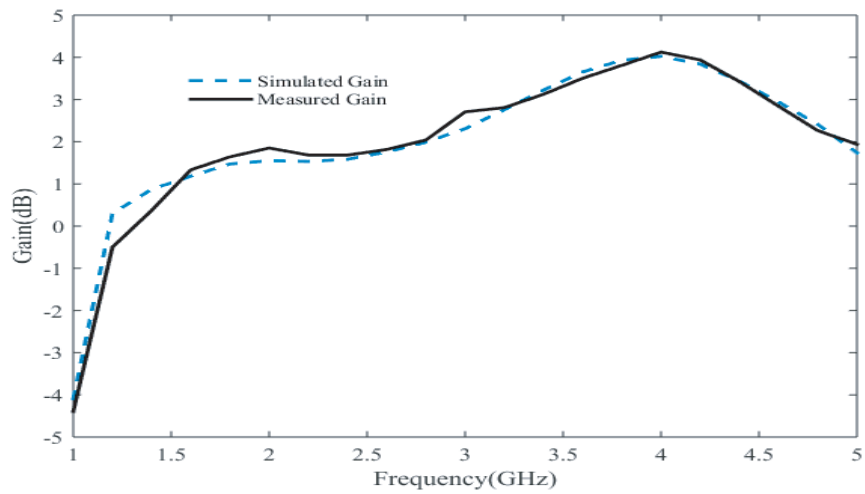


Figure 16. Simulated and measured gain of the proposed antenna.

#### 4. RESULTS AND DISCUSSION

The proposed wideband antenna performance was discussed. The electrical performance parameters of the proposed antenna were measured by Anritsu MS2037C/2 network analyzer. The prototype of antenna is presented in Figure 14.

The simulated and measured results of  $S_{11}$  are shown in Figure 15. The proposed antenna achieves 81% of wide impedance bandwidth with  $S_{11} < -10$  dB from 1.6 GHz to 3.8 GHz. The results of the antenna gain are 1.5 dBi and 2.5 dBi maintained at 1.8 GHz and 3.3 GHz as shown in Figure 16.

2-D radiation patterns of the proposed antenna are shown in Figure 17 at resonant frequencies 1.8 GHz and 3.3 GHz. In Figure 17, tilting of radiation pattern at 3.3 GHz frequency from  $0^\circ$  to  $60^\circ$  in  $yo$  $z$ -plane is observed due to increased magnitude of higher order mode. The radiation patterns in the  $yo$  $z$ -plane and  $xo$  $z$ -plane are nearly stable over the wide frequency band with omnidirectional and nearly monopole-like shape.

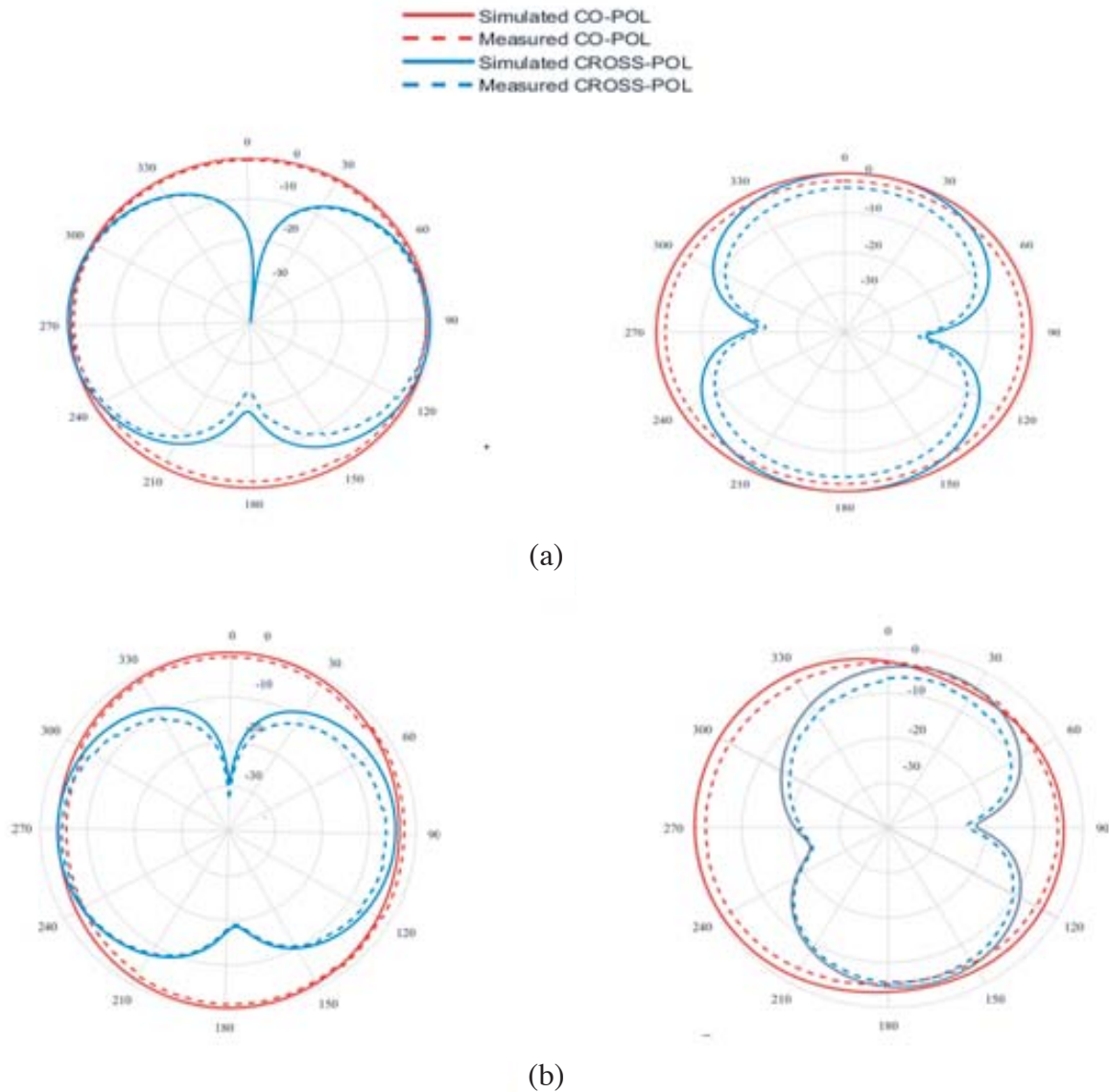


**Figure 17.** Simulated and measured radiation patterns at (a) 1.8 GHz and (b) 3.3 GHz.

## 5. CONCLUSION

The CMA has been engaged to design a new wideband antenna. The antenna design is analyzed through the concept of desired two modes excitation at once with a simple feeding structure to broaden the impedance bandwidth. The wide impedance bandwidth of 81% ( $|S_{11}| < -10$ ) from 1.6 to 3.8 GHz is achieved for both the simulated and measured results.

## REFERENCES

1. Balanis, C. A., *Antenna Theory: Analysis and Design*, 3rd edition, Wiley, New York, NY, USA, 2005.
2. Rumsey, V., "Frequency independent antennas," *IRE International Convention Record*, Vol. 5, 114–118, 1957.
3. DuHamel, R. and F. Ore, "Logarithmically periodic antenna designs," *IRE International Convention Record*, Vol. 6, 139–151, IEEE, 1958.
4. Dyson, J., "The characteristics and design of the conical log spiral antenna," *IEEE Transactions on Antennas and Propagation*, Vol. 13, No. 4, 488–499, Apr. 1965.
5. Sharma, S. K., L. Shafai, and N. Jacob, "Investigation of wide-band microstrip slot antenna," *IEEE Transactions on Antennas and Propagation*, Vol. 52, No. 3, 865–872, Mar. 2004.
6. Garbacz, R., "Modal expansions for resonance scattering and phenomena," *Proc. IEEE*, Vol. 53, 856–864, Aug. 1965.
7. Khan, M. and D. Chatterjee, "Characteristic mode analysis of a class of empirical design techniques for probe-fed, U-slot microstrip patch antennas," *IEEE Transactions on Antennas and Propagation*, Vol. 64, No. 7, 2758–2770, Jul. 2016.
8. Mohamed-Hicho, N. M., E. Antonino-Daviu, M. Cabedo-Fabrés, and M. Ferrando-Bataller, "Designing slot antennas in finite platforms using characteristic modes," *IEEE Access*, Vol. 6, 41346–41355, 2018.
9. Antonino-Daviu, E., M. Cabedo-Fabrés, M. Sonkki, N. M. Mohamed-Hicho, and M. Ferrando-Bataller, "Design guidelines for the excitation of characteristic modes in slotted planar structures," *IEEE Transactions on Antennas and Propagation*, Vol. 64, No. 12, 5020–5029, Dec. 2016.
10. Khan, M. and D. Chatterjee, "Analysis of reactive loading in a U-slot microstrip patch using the theory of characteristic modes," *IEEE Antennas & Propagation Magazine*, Vol. 60, No. 6, 88–97, Dec. 2018.
11. Ghalib, A., R. Hussain, and M. S. Sharawi, "Analysis of slot-based radiators using TCM and its application in MIMO antennas," *International Journal of RF and Microwave Computer-Aided Engineering*, e21544, 2018.
12. Li, K. and Y. Shi, "A pattern reconfigurable MIMO antenna design using characteristic modes," *IEEE Access*, 2018, doi: 10.1109/ACCESS.2018.2863250.
13. Won, J., S. Jeon, and S. Nam, "Identifying the appropriate position on the ground plane for MIMO antennas using characteristic mode analysis," *Journal of Electromagnetic Engineering and Science*, Vol. 16, No. 2, 119–125, Apr. 2016.
14. Antonino-Daviu, E., M. Cabedo-Fabrés, M. Ferrando-Bataller, and M. Gallo, "Design of a multimode MIMO antenna using the theory of characteristic modes," *Radio Engineering*, Vol. 18, No. 4, 425–430, Dec. 2009.
15. Zhang, Q., Q. Zhang, and Y. Gao, "Design of a multi-mode UWB antenna using characteristic mode analysis," *IEEE Transactions on Antennas and Propagation*, Vol. 66, No. 7, 3712–3717, Jul. 2018.
16. Zhang, Q. and Y. Gao, "Compact low-profile UWB antenna with characteristic mode analysis for UHF TV white space devices," *IET Microwaves, Antennas & Propagation*, Vol. 11, No. 11, 1629–1635, 2017.

17. Wu, W. and Y. P. Zhang, "Analysis of ultra-wideband printed planar quasi-monopole antennas using the theory of characteristic modes," *IEEE Antennas and Propagation Magazine*, Vol. 52, No. 6, 67–77, Dec. 2010.
18. Ma, R., T.-Y. Shih, R. Lian, and N. Behdad, "Design of bandwidth-enhanced, platform-mounted, electrically-small VHF antennas using the characteristic-mode theory," *IEEE Antennas and Wireless Propagation Letters*, Vol. 17, No. 12, 2384–2388, Dec. 2018.
19. Wang, C., Y. Chen, and S. Yang, "Application of characteristic mode theory in HF band aircraft-integrated multi-antenna system design," *IEEE Transactions on Antennas and Propagation*, Vol. 67, No. 1, 513–521, Jan. 2019.
20. Li, M. and N. Behdad, "Design of a dual-band platform-mounted HF/VHF antenna using the characteristic modes theory," *2017 11th European Conference on Antennas and Propagation (EUCAP)*, 3461–3463, 2017.
21. Chen, Y. and C.-F. Wang, "Electrically small UAV antenna design using characteristic modes," *IEEE Transactions on Antennas and Propagation*, Vol. 62, No. 2, 535–545, Feb. 2014.
22. Li, T. and Z. N. Chen, "Metasurface-based shared-aperture 5G S/K-band antenna using characteristic modes analysis," *IEEE Transaction on Antennas and Propagation*, Vol. 66, No. 12, 6742–6750, 2018.
23. Santillán-Haro, D., E. A. Daviu, D. S. Escuderos, and M. F. Bataller, "Analysis and design of a metamaterial lens antenna using the theory of characteristic modes," *International Journal of Antennas and Propagation*, Vol. 2018, Article ID 6329531, 8 pages, 2018.
24. Li, T. and Z. N. Chen, "A dual-band metasurface antenna using characteristic mode analysis," *IEEE Transactions on Antennas and Propagation*, Vol. 66, No. 10, 5620–5624, Oct. 2018.
25. Lin, F. H. and Z. N. Chen, "Truncated impedance-sheet model for low-profile broadband non-resonant-cell metasurface antennas using characteristic mode analysis," *IEEE Transactions on Antennas and Propagation*, Vol. 66, No. 10, 5043–5051, Oct. 2018.
26. Lin, F. H. and Z. N. Chen, "A method of suppressing higher order modes for improving radiation performance of metasurface multipoint antennas using characteristic mode analysis," *IEEE Transactions on Antennas and Propagation*, Vol. 66, No. 4, 1894–1902, Apr. 2018.
27. Saraswat, K. and A. R. Harish, "Analysis of wideband circularly polarized ring slot antenna using characteristics mode for bandwidth enhancement," *International Journal of RF and Microwave Computer-Aided Engineering*, e21186, 2017.
28. Wen, D., Y. Hao, H. Wang, and H. Zhou, "Design of a wideband antenna with stable omnidirectional radiation pattern using the theory of characteristic modes," *IEEE Transactions on Antennas and Propagation*, Vol. 65, No. 5, 2671–2676, May 2017.
29. Wang, C., Y. Chen, and S. Yang, "Bandwidth enhancement of a dual-polarized slot antenna using characteristic mode," *IEEE Antennas and Wireless Propagation Letters*, Vol. 17, No. 6, 988–992, Jun. 2018.
30. Wen, D., Y. Hao, H. Wang, and H. Zhou, "Design of a wideband antenna by manipulating characteristic modes of a metallic loop," *Microwave and Optical Technology Letters*, 1–6, 2018.
31. Lin, F. H. and Z. N. Chen, "Low-profile wideband metasurface antennas using characteristic mode analysis," *IEEE Transactions on Antennas and Propagation*, Vol. 65, No. 4, 1706–1713, Apr. 2017.
32. Liang, Z., J. Ouyang, and F. Yang, "Design and characteristic mode analysis of a low-profile wideband patch antenna using metasurface," *Journal of Electromagnetic Waves and Applications*, Vol. 32, No. 17, 2304–2313, 2018.
33. Yang, X., Y. Lin, and S.-X. Gong, "Design of wideband omnidirectional antenna with characteristic mode analysis," *IEEE Antennas and Wireless Propagation Letters*, Vol. 17, No. 6, 993–997, Jun. 2018.
34. Zhao, C. and C.-F. Wang, "Characteristic mode design of wide band circularly polarized patch antenna consisting of H-shaped unit cells," *IEEE Access*, Vol. 6, 25292–25299, Apr. 20, 2018.
35. Garbacz, R. J. and R. H. Turpin, "A generalized expansion for radiated and scattered fields," *IEEE Transactions on Antennas and Propagation*, Vol. 19, No. 3, 348–358, Mar. 1971.

36. Harrington, R. F. and J. R. Mautz, "The theory of characteristic modes for conducting bodies," *IEEE Transactions on Antennas and Propagation*, Vol. 19, No. 5, 622–628, May 1971.
37. Harrington, R. F. and J. R. Mautz, "Computation of characteristic modes for conducting bodies," *IEEE Transactions on Antennas and Propagation*, Vol. 19, No. 5, 629–639, May 1971.
38. Cabedo-Fabres, M., E. Antonino-Daviu, A. Valero-Nogueira, and M. F. Bataller, "The theory of characteristic modes revisited: A contribution to the design of antennas for modern applications," *IEEE Antennas and Propagation Magazine*, Vol. 49, No. 5, 52–68, Oct. 2007.
39. Lau, B. K., D. Manteuffel, H. Arai, and S. V. Hum, "Guest editorial theory and applications of characteristic modes," *IEEE Transactions on Antennas and Propagation*, Vol. 64, No. 7, 2590–2594, Jul. 2016.
40. Vogel, M., G. Gampala, D. Ludick, U. Jakobus, and C. J. Reddy, "Characteristic mode analysis: Putting physics back into simulation," *IEEE Antennas and Propagation Magazine*, Vol. 57, No. 2, 307–317, Apr. 2015.
41. Li, W., Y. Liu, J. Li, L. Ye, and Q. H. Liu, "Modal proportion analysis in antenna characteristic mode theory," *International Journal of Antennas and Propagation*, Vol. 2019, Article ID 7069230, 10 pages, 2019.
42. Strang, G., "Linear algebra and its applications," *Cengage Learning*, 2006.
43. Koliha, J. J., "Block diagonalization," *Mathematica Bohemica*, Vol. 126, No. 1, 237–246, 2001.